

IEICE Proceeding Series

A Simple Chaotic Circuit Based on Coupled Spiking Neurons

Shinya Tanaka, Toshimichi Saito, Kunihiko Mitsubori

Vol. 1 pp. 899-902

Publication Date: 2014/03/17

Online ISSN: 2188-5079

Downloaded from www.proceeding.ieice.org

©The Institute of Electronics, Information and Communication Engineers

A Simple Chaotic Circuit Based on Coupled Spiking Neurons

Shinya Tanaka, Toshimichi Saito

EE Dept., HOSEI University
 Koganei, Tokyo, 184-8584 Japan
 {shinya.tanaka.8k@stu., tsaito@}hosei.ac.jp

Kunihiko Mitsubori

ECS Dept., Takushoku University
 Hachioji, Tokyo, 193-0985 Japan
 mitubori@es.takushoku-u.ac.jp

Abstract— This paper studies chaotic spiking oscillators with two integrate-and-fire switches. The circuit has signum activation function and piecewise constant vector field that is well suited for precise analysis. The two firing switches can cause interesting chaotic behavior that is hard in the case of one firing switch. Using the piecewise linear return map, the dynamics can be analyzed precisely. Presenting a simple test circuit, typical phenomena are confirmed in laboratory.

I. INTRODUCTION

Spiking signals play important roles in a variety of artificial/biological systems. Basically, the spiking signals are generated by integrate-and-fire switching (IFS). The IFS is a key element in various nonlinear circuits and systems such as spiking neurons and chaotic spiking oscillators [1]-[6]. The IFS resets a state variable when it reaches a threshold. Repeating the integrate-and-fire behavior, the system can output a variety of chaotic/periodic spike-trains and related bifurcation phenomena [2][6]. The spiking neurons can be a building block of pulse-coupled neural networks having rich synchronous phenomena. Analysis of the spike-trains is basic to consider information processing function in the brain [7] and spike-based engineering applications including image /signal processing [8], ultra wide-band communications [9] and neural prosthesis [10]. Analysis of the IFS-based dynamics is important for development of neuroscience, chaos-bifurcation theory and engineering applications.

This paper studies chaotic spiking oscillators (CSO) consisting of two capacitors, two voltage-controlled voltage sources (VCCS) and two IFSs. Noted that this is the first paper of CSO with two IFSs although there are many papers of the CSO with one IFS [11]-[17]. In the circuit equation, the VCCS is modeled by signum function that makes the vector field piecewise constant (PWC [18]). The trajectory is piecewise linear (PWL) and the return map is also PWL. The trajectory can rotate divergently around the origin. If either capacitor voltage reaches the threshold, either IFS resets the voltage to the base level. The rotation and two IFSs can cause a variety of chaos and bifurcation phenomena and this paper demonstrates typical phenomena: chaos by two IFSs with rotation, chaos by two IFSs without rotation and their

transition. Such phenomena are impossible in the CSO with one IFS in [11]-[17]. Typical phenomena are analyzed precisely by the PWL return map that is a strong analysis tool. Presenting a simple test circuit, typical phenomena are confirmed experimentally.

II. CHAOTIC SPIKING OSCILLATORS

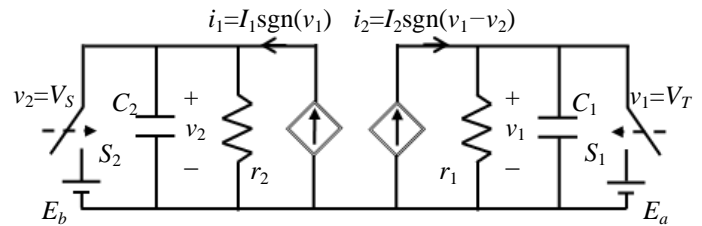


Fig.1 Objective circuit model.

Fig.1 shows the objective circuit model. This circuit consists of two capacitors C_1 and C_2 , two voltage-controlled current sources (VCCSs), and two firing switches S_1 and S_2 , with two base voltages E_a and E_b . Each VCCS is characterized by the signum function: $\text{sgn}(v) = 1$ for $v \geq 0$, -1 for $v < 0$. For simplicity, we assume that the two inner resistors r_1 and r_2 are large enough and we regard them as open. If both switches are open, this circuit dynamics is described by

$$C_1 \frac{dv_1}{dt} = I_2 \text{sgn}(v_1 - v_2), \quad C_2 \frac{dv_2}{dt} = I_1 \text{sgn}(v_1). \quad (1)$$

The switches S_1 and S_2 are controlled by either of the following three rules.

Rule A1: S_2 is open all the time. S_1 is closed and v_1 is reset to E_a instantaneously if v_1 reaches the threshold voltage $V_T > 0$.

$$(v_1(t_+), v_2(t_+)) = (E_a, v_2(t)) \quad \text{if } v_1(t) = V_T. \quad (2)$$

Rule A2 S_1 is open all the time. S_2 is closed and v_2 is reset to E_b instantaneously if v_2 reaches the threshold voltage $V_s > 0$.

$$(v_1(t_+), v_2(t_+)) = (v_1(t), E_b) \quad \text{if } v_2(t) = V_s. \quad (3)$$

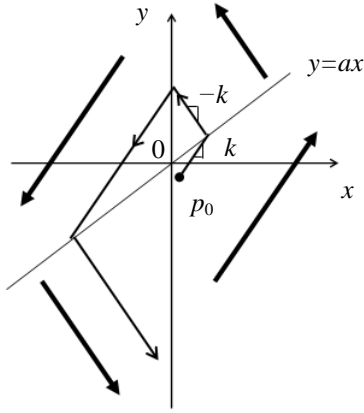


Fig.2 Example of the trajectory.

Rule B is a combination of Rules A1 and A2: S_1 is controlled by Eq. (2) and S_2 controlled by Eq. (3). (S_1 and S_2 are not fixed to be open all the time).

Using dimensionless variables and parameters:

$$\tau = (I_2 t)/(C_1 V_T), \quad x = v_1/V_T, \quad y = v_2/V_S, \quad a = V_T/V_S, \\ b = (C_1 I_1)/(C_2 I_2), \quad q_a = E_a/V_T, \quad q_b = E_b/V_S, \quad k = ab, \quad (4)$$

Equations (1), (2) and (3) are transformed into

$$\frac{dx}{d\tau} = \text{sgn}(ax - y), \quad \frac{dy}{d\tau} = k \text{sgn}(x). \quad (5)$$

$$\text{Rule A1: } (x(\tau_+), y(\tau_+)) = (q_a, y(\tau)) \quad \text{if } x(\tau) = 1. \quad (6)$$

$$\text{Rule A2: } (x(\tau_+), y(\tau_+)) = (x(\tau), q_b) \quad \text{if } y(\tau) = 1. \quad (7)$$

Rule B: combination of Rules A1 and A2.

Hereafter, we consider the case where $0 < a < k$. Fig.2 shows the example of the trajectory of Equation (5) where the firing switches S_1 and S_2 are open all the time. The trajectory “rotates” divergently around the origin, and it draws “rect-spiral”. The signum function makes the trajectory PWL and the borders are two lines $x=0$ and $y=ax$. For example, in the region $x > 0$ and $y < ax$, the trajectory draws a line with slope k . If it hits the line $y = ax$, it enters the region where $y > ax$ and draws a line with slope $-k$. Repeating this manner, the trajectory draws the rect-spiral. If the trajectory hits either the threshold $x = 1$ (respectively, $y = 1$), then it jumps horizontally to the base $x = q_a$ (respectively, vertically to the base $y = q_b$).

Figure 3 shows the typical trajectories in the rules A1, A2, and B. The parameters have the same values for the three rules. Note that the case of one switch (rule A1 or A2) has been discussed in our previous works, however, the case of two switches (rule B) has not been discussed. In Fig.3 (a) of rule A1, the trajectory repeats the horizontal jumps and exhibits chaotic attractor. A theoretical evidence for chaos generation (positive-ness of Lyapunov exponent) can be found in [16]. In Fig. 3(b) of rule A2, the trajectory repeats vertical jumps and it diverges. In Fig. 3 (c) of rule B, the trajectory repeats the both horizontal and vertical jumps, and exhibit chaotic attractor without “rotation” around the origin. Such chaotic behavior is impossible in the system with one switching.. The rule B can cause a variety of chaos and bifurcation.

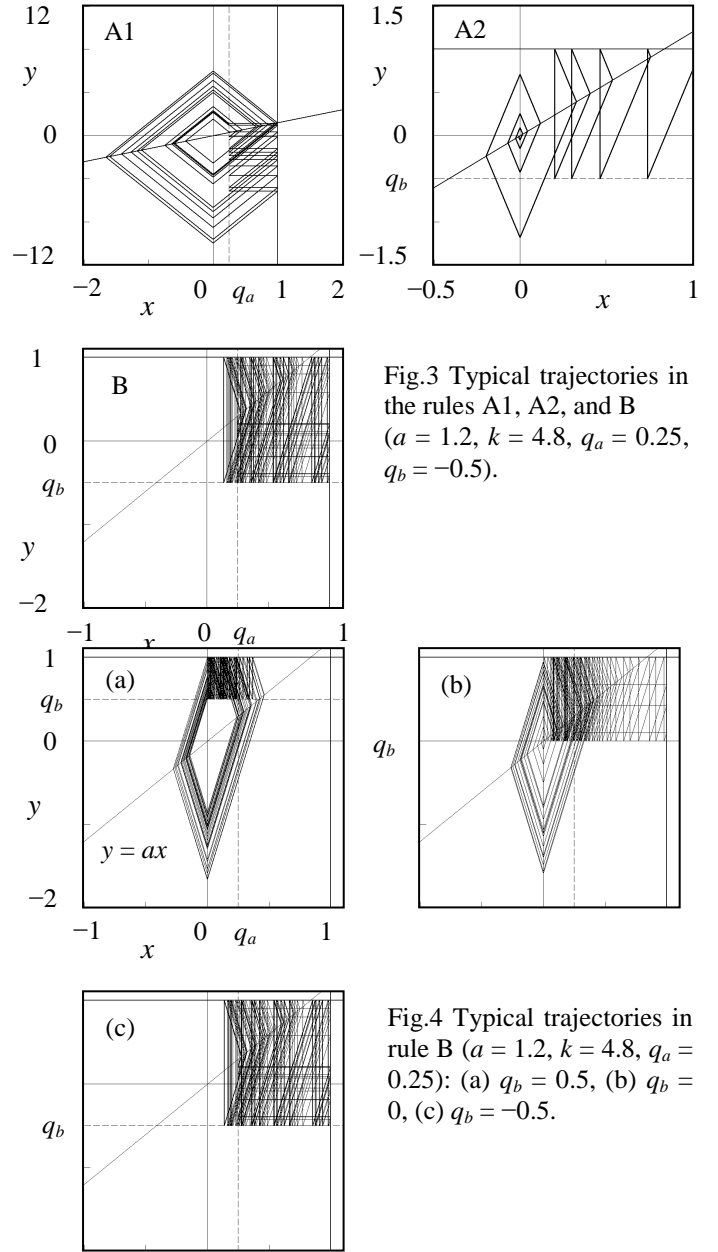


Fig.3 Typical trajectories in the rules A1, A2, and B ($a = 1.2, k = 4.8, q_a = 0.25, q_b = -0.5$).

Fig.4 Typical trajectories in rule B ($a = 1.2, k = 4.8, q_a = 0.25$): (a) $q_b = 0.5$, (b) $q_b = 0$, (c) $q_b = -0.5$.

Hereafter, we focus on the case of rule B described by Eqs. (5) to (7): two kinds of thresholds and jumps. Fig.4 shows typical phenomena. Figure 4 (a) shows chaos with vertical jump. As q_b decreases (the left parameter values are fixed) this attractor is changed into chaotic behavior in Figs. 4 (b) and (c). In (b) the trajectory rotates divergently around the origin, it repeats switchings in y -direction, jumps to the base in x -direction. We refer to it as “chaos by 2 integrate-and-fire switchings (IFSs) with rotation”. In (c), the trajectory exhibits jumps with both x - and y -directions and draws chaotic attractor without rotation around the origin. We refer to it as “chaos by two IFSs without rotation”. System with one IFS can not exhibit chaotic attractor in (b), that in (c) and related bifurcation. In Sections III and IV, these phenomena are investigated by PWL return maps and in laboratory experiments, respectively.

III. PIECEWISE LINEAR RETURN MAP

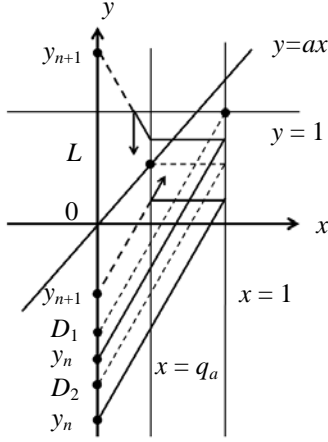


Fig.5 Definition of 1-D return map in phase plane.

In order to analyze these phenomena, we derive a 1D return map. This paper focuses on the following parameter regions:

$$\begin{aligned} PR_1 &= \{(a, q_a, q_b) \mid a \geq 1, 0 \leq q_a \leq 1, 0 \leq q_b \leq 1\}, \\ PR_2 &= \{(a, q_a, q_b) \mid a \geq 1, 0 \leq q_a \leq 1, q_b \leq 0\}. \end{aligned} \quad (8)$$

The phenomena in Fig.4 are observed in these regions. Fig.5 shows the example of the trajectory from the circuit. Let $L = \{(x, y) \mid x = 0\}$, and let a point on L be represented by its y -coordinate. Since the trajectory starting from L returns to L at some positive time, we can define the 1D return map f from L to L itself. Letting y_0 and y_n denote the initial point on L and the n -th return point on L , the dynamics can be integrated into iteration of f :

$$f : L \mapsto L, y_{n+1} = f(y_n). \quad (9)$$

If we use this definition straightforwardly, the calculation of the image of this map is complicated because the domain L is divided into many subintervals. In order to avoid this complication, we define an ‘‘imaginary point’’ as the following.

Definition: The trajectory hitting the threshold $y = 1$ in the region $y > ax$ often does not return L immediately. In this case, we neglect the threshold to extend the trajectory, and we define a point which this trajectory hits on L as the image of the map. Letting $L' = \{(x, y) \mid x = 0, y > 1\}$, this point is on L' and the actual trajectory does not hit it. We refer to this point as the ‘‘imaginary point’’.

Next, we define the important points to consider this map. Let $D_1 \in L$ denote a point such that a trajectory starting from D_1 hits $(x, y) = (1, 1)$. Let $D_2 \in L$ denote a point such that a trajectory starting from D_2 hits the threshold $x = 1$ and it jumps to $(x, y) = (q_a, aq_a)$. Let $D_3 \in L$ denote a point such that a trajectory starting from D_3 passes $(x, y) = (1/a, 1)$. Let $B \in L' \subset L$ denote a point such that a trajectory starting from B passes $(x, y) = (q_b/a, q_b)$. These points are given by

$$D_1 = 1 - k, \quad D_2 = aq_a - k, \quad D_3 = 1 - \frac{k}{a}, \quad D_4 = \frac{a - k}{a + k}. \quad (10)$$

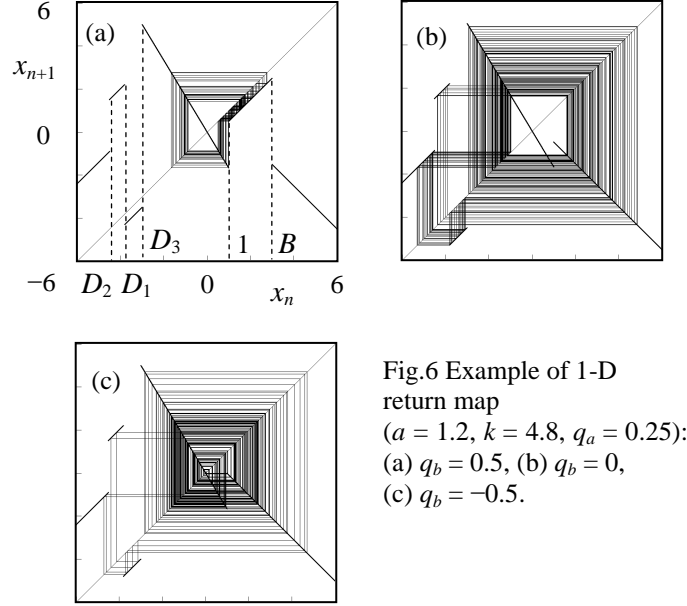


Fig.6 Example of 1-D return map ($a = 1.2, k = 4.8, q_a = 0.25$): (a) $q_b = 0.5$, (b) $q_b = 0$, (c) $q_b = -0.5$.

We explain the connection of the trajectory and the image of the map. For example, we consider the case where $(a, q_a, q_b) \in PR_1$ and $y_n < D_1$. Fig.5 corresponds to this case. If $D_2 < y_n < D_1$, the trajectory starting from y_n hits the threshold $x = 1$ and it jumps to $x = q_a$ horizontally. This trajectory hits the threshold $y = 1$ and it jumps to $y = q_b$ vertically. It does not return L immediately. In this case, we define y_{n+1} as the imaginary point. If $y_n < D_2$, the trajectory starting from y_n hits the threshold $x = 1$ and it jumps to $x = q_a$ horizontally. It does not return L immediately. In this case, we define y_{n+1} as a point such that the trajectory after this horizontal jump coincides with the one starting from y_{n+1} . By using the same manner, we can define y_{n+1} for $D_1 < y_n$. According to the similar procedures, we can derive this return map for $(a, q_a, q_b) \in PR_2$. This return map is piecewise linear, and is described explicitly by the following simple formula:

$$y_{n+1} = f(y_n) = \begin{cases} y_n + k - kq_a & \text{for } y_n \leq D_2 \\ y_n + k + kq_a & \text{for } D_2 < y_n < D_1 \\ y_n + q_b - 1 & \text{for } D_1 \leq y_n \leq D_3 \\ (a+k)y_n / (a-k) & \text{for } D_3 < y_n < 1 \\ y_n + q_b - 1 & \text{for } 1 \leq y_n < B \\ -y_n + q_b + 1 & \text{for } B \leq y_n \end{cases} \quad (11)$$

for $(a, q_a, q_b) \in PR_1$ and

$$y_{n+1} = f(y_n) = \begin{cases} y_n + k - kq_a & \text{for } y_n \leq D_2 \\ y_n + k + kq_a & \text{for } D_2 < y_n < D_1 \\ y_n + q_b - 1 & \text{for } D_1 \leq y_n < D_3 \\ (a+k)y_n / (a-k) & \text{for } D_3 < y_n < 1 \\ -y_n + q_b + 1 & \text{for } 1 \leq y_n \end{cases} \quad (12)$$

for $(a, q_a, q_b) \in PR_2$. Fig.6 shows the example of this 1-D return map. The map (a), (b), and (c) in Fig.6 corresponds to the attractors in Fig.4 (a), (b), and (c), respectively.

IV. EXPERIMENTS

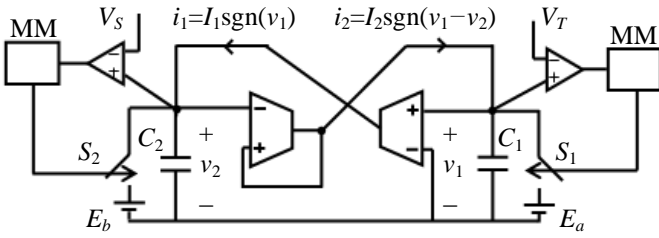


Fig.7 Test circuit.

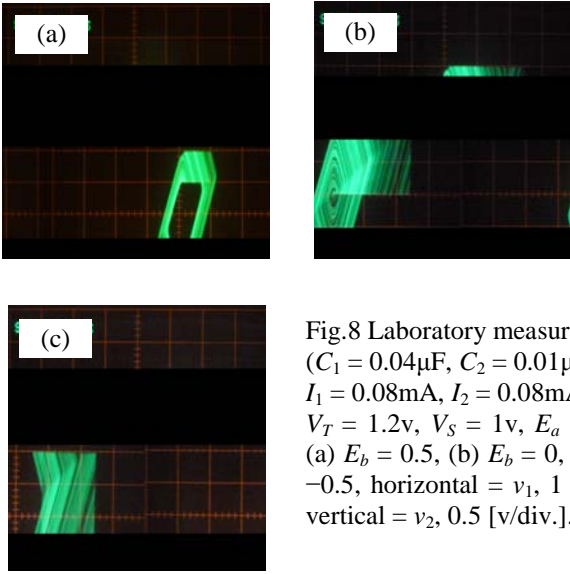


Fig.8 Laboratory measurements ($C_1 = 0.04\mu\text{F}$, $C_2 = 0.01\mu\text{F}$, $I_1 = 0.08\text{mA}$, $I_2 = 0.08\text{mA}$, $V_T = 1.2\text{V}$, $V_S = 1\text{V}$, $E_a = 0.3\text{V}$): (a) $E_b = 0.5$, (b) $E_b = 0$, (c) $E_b = -0.5$, horizontal = v_1 , 1 [v/div.], vertical = v_2 , 0.5 [v/div.].

We have fabricated a simple test circuit as shown in Fig.7. VCCSs are realized by OTAs (LM13600). If each voltage of the capacitor reaches the threshold, the comparator (LM339) triggers the mono-stable multi-vibrator MM (4538) to close each switch, and then the voltage is reset to the base. Each switch is realized by an analog switch (4066). Fig.8 shows the laboratory measurements from this test circuit. The attractors in Fig.8 (a), (b), and (c) corresponds to the ones in Fig.4 (a), (b), and (c), respectively.

V. CONCLUSIONS

The CSOs with two IFSs have been studied in this paper. The circuit can cause double-switching chaotic phenomena that are impossible in the case of one IFS. For a systematic and precise analysis, one-dimensional PWL return map is formulated explicitly. Typical phenomena are analyzed precisely and confirmed in the laboratory.

Future problems are many, including classification of phenomena, analysis of bifurcation phenomena, development

into artificial spiking neurons and engineering applications. Note that the system analysis is in progress and the demonstrated phenomena in this paper are "the tip of the iceberg".

REFERENCES

- [1] J. P. Keener, F. C. Hoppensteadt and J.-Rinzel, "Integrate-and-fire models of nerve membrane response to oscillatory input", *SIAM J. Appl. Math.*, 41, pp. 503-517, 1981.
- [2] R. Perez and L. Glass, "Bistability, period doubling bifurcations and chaos in a periodically forced oscillator", *Phys. Lett.*, 90A, 9, pp. 441-443, 1982.
- [3] R. E. Mirollo and S. H. Strogatz, "Synchronization of pulse-coupled biological oscillators", *SIAM J. Appl. Math.*, 50, 6, pp.1645-1662, 1990.
- [4] E. M. Izhikevich, "Resonate-and-fire neurons", *Neural Networks*, 14, pp. 883-894, 2001.
- [5] E. M. Izhikevich, "Simple Model of Spiking Neurons", *IEEE Trans. Neural Networks*, 14, pp. 1569-1572, 2003.
- [6] Y. Yamashita and H. Torikai, "Bursting Analysis and Synapse Mechanism of A Piece-wise Constant Spiking Neuron Model", *Proc. IJCNN*, pp. 193-200, 2012.
- [7] T. Toyozumi, K. Aihara and S. Amari, "Fisher information for spike-based population coding", *Phys. Rev. Lett.*, 97, 098102, 2006.
- [8] S. R. Campbell, D. Wang and C. Jayaprakash, "Synchrony and desynchrony in integrate-and-fire oscillators", *Neural computation*, vol. 11, pp. 1595-1619, 1999.
- [9] G. M. Maggio, N. Rulkov and L. Reggiani, "Pseudo-Chaotic Time Hopping For UWB Impulse Radio", *IEEE Tran. Circuits Syst.*, I, 48, 12, pp. 1424-1435, 2001.
- [10] S. Hashimoto and H. Torikai, "A Novel Hybrid Spiking Neuron: Bifurcations, Responses, and On-Chip Learning", *IEEE Trans. Circuits Syst. I*, 57, 8, pp. 2168-2181, 2010.
- [11] K. Mitsubori and T. Saito, "Dependent switched capacitor chaos generator and its synchronization", *IEEE Trans. Circuits Syst. I*, 44, 12, pp. 1122-1128, 1997.
- [12] K. Mitsubori and T. Saito, "Mutually Pulse-coupled Chaotic Circuits by using Dependent Switched Capacitors", *IEEE Trans. Circuits Syst. I*, 47, 10, pp. 1469-1478, 2000.
- [13] H. Nakano and T. Saito, "Basic dynamics from a pulse-coupled network of autonomous integrate-and-fire chaotic circuits", *IEEE Trans. Neural Networks*, 13, 1, pp. 92-100, 2002.
- [14] Y. Takahashi, H. Nakano and T. Saito, "A simple hyperchaos generator based on impulsive switching", *IEEE Trans. Circuits Syst. II*, 51, 9, pp. 468-472, 2004.
- [15] H. Nakano and T. Saito, "Grouping synchronization in a pulse-coupled network of chaotic spiking oscillators", *IEEE Trans. Neural Networks*, 15, 5, pp. 1018-1026, 2004.
- [16] Y. Matsuoka and T. Saito, "A Simple Chaotic Spiking Oscillator Having Piecewise Constant Characteristics", *IEICE Trans. Fundamentals*, 89, 9, pp. 2437-2440, 2006.
- [17] Y. Matsuoka, T. Hasegawa and T. Saito, "Chaotic Spike-train with Line-like Spectrum", *IEICE Trans. Fundamentals*, E92-A, 4, pp. 1142-1147, 2009.
- [18] T. Tsubone and T. Saito, "Manifold piecewise constant systems and chaos", *IEICE Trans. Fundamentals*, E82-A, 8, pp.1619-1626, 1999.